JTE HCMUTE
ISSN: 2615-9740

JOURNAL OF TECHNICAL EDUCATION SCIENCE
Ho Chi Minh City University of Technology and Education
Website: https://jte.edu.vn
Email: jte@hcmute.edu.vn

On Research of Cable Tension Distribution Algorithm for Four Cables - Three DOF Planar Cable-Driven Parallel Robot

Cong Hoang Kha Dao, Phuoc Tho Tuong*, Ngoc Duc Vu, Minh Nhat Nguyen
Ho Chi Minh City University of Technology and Education, Vietnam

*Corresponding author. *Email: thotp@hcmute.edu.vn*

ARTICLE INFO

Received: 21/11/2022
Revised: 13/01/2023
Accepted: 23/02/2023
Published: 28/08/2023

KEYWORDS

Tension distribution algorithm;
Cable-driven parallel robot;
Quadratic programming;
Over-constraint CDPR;
3 DOF parallel robot.

ABSTRACT

One of the main concerns in controlling the cable-driven parallel robot (CDPR) mechanism is dealing with the distribution of tension on each cable, which is critical to the operation of the entire cable system. It can be said that adjusting the cable tension will determine the power consumption of the motors and the stiffness of the structure. Therefore, the problem that needs to be solved is how to handle the cable tension when the end-effector moves throughout the entire workspace. The tension of each cable needs to be adjusted properly to ensure it remains the same. Moment and force act in a static state, keeping the kinematic position of the end moving platform from being deflected and the main purpose is to ensure that the robot achieves a rigid state and eliminates vibration when moving. Because of that essential demand, this article will refer to the Quadratic programming algorithm to solve the problem of tension distribution for the Planar Cable-Driven Parallel Robot consisting of 4 cables with 3 degrees of freedom. This article will be the foundation for applying this algorithm to an 8-cable robot with 6 degrees of freedom (Spatial Cable-Driven Parallel Robot for example). At the same time, in this article, the simulation results for the algorithm will also be presented in this paper.

Doi: https://doi.org/10.54644/jte.78B.2023.1312

1. Introduction

Cable-driven parallel robot (CDPR) is a type of parallel robot that uses the cable to control the end effector (E-E) instead of using rigid joints. One of the main advantages of CDPR is the ability to create a large workspace while maintaining high stiffness and low inertness. Low cost for large workspaces is also a notable advantage [1]. Thanks to the advantages of CDPR, it can be used in many research fields like rehabilitation, haptic, movement simulation, and 3D printing..... The feature of tension distribution for CDPRs is one of the most considerations in designing, and controlling the problem of CDPRs. Tension involves issues such as system balancing, feasible workspace determination, actuator power, mechanism stiffness, trajectory movement, and controller design [2]. Many proposed methods of tension distribution have been conveyed in the research of CDPR, Tuong Phuoc Tho and Nguyen Truong Thinh [3] used linear optimization to find the solution of tension distribution for the CDPR used for 3D concrete printing, under high-load working conditions and long working hours, reducing power consumption is paramount to save energy, because printing velocity is slow, dynamic effects are ignored. Besides, Cong Bang Pham et al [4] also used the “Linear Optimization” algorithm to build the calculation of cable tension. So-Ryeok Oh and Sunil K. Agrawal [5] applied the proposed “Linear Optimization” method to find cable tension for PM-CDPR form, the results were simulated successfully. Based on these models, all authors also develop an algorithm to control the robot by providing negative tension. Soon after, Per Henrik Borgstrom et al. [6] made improvements to the “Linear Programming” algorithm to simplify the calculation process applied for tension distribution. In the specific case where the positive tension aggregation method has been selected to finalize the optimal solutions and the optimal criterion.

Similar to the Linear Programming algorithm, the Non-linear Programming algorithm has been applied to find the tension distribution of the cables. The disadvantage of Linear Programming is the discontinuous tension distribution along the joint trajectory. A new Quadratic Programming method has

been concerned (p-norm = 2) [5] [7], which is a quadratic objective function form, this gives continuity of root force due to the ability to restrict the vertices of the convex polygon (the set of the experiment). Tobias Bruckmann et al. [8] introduce Quadratic Programming for determining cable tension solutions for FC-CDPRs or OC-CDPRs. The quadratic objective function provided a better computation time than the linear form. Hui Li et al. [9] applied Quadratic Programming to research the problem of tension solution for the FAST telescope. In another study [10], the author found that a non-linear cost function can optimize cable tension to save power consumption. Alexis Fortin Cote et al. [11] also use Quadratic Programming to find tension distribution with the belief of a second optimal solution by adding another parametric slack variable into the force equilibrium equation, this is likely to solve the tensile distribution even outside the workspace.

The analysis of the above studies shows that many methods have been developed to calculate the distribution of cable tension for the over-constraint CDPR. These methods focus on optimizing solutions according to different goals, such as stress reduction for applications requiring energy savings and safe tension for convenient control or maximum tension to increase structural rigidity. The Linear Programming method gives discontinuous results according to the joint trajectory, while the Quadratic Programming Methods methods result in continuous cable tensions according to the motion trajectory and can be adjusted for optimal conditions. Given the inertia and low mass of the cables, these mechanisms have the disadvantage that they can only support traction, which increases the complexity of calculating the tension distribution for a given position of the End-Effector (E-E). Besides, the cable factor also affects the direction limit of E-E, which also creates difficulties because we have to eliminate the impossible sequences of direct operation on E-E at E-E at each position in the robot workspace. To find the position of E-E, the kinematics problem must be solved. This article focuses on in-depth research on the algorithm for cable tension distribution of the Over constraint planar CDPR type. Based on the studies on tension distribution [3-11], we will design and analyze the Quadratic Programming algorithm and simulate each position of E-E to evaluate and comment on the accuracy of the properties of the cable tension. At the same time, this article also analyzes an important part of the kinematics for this type of robot, including forward and inverse kinematics. The limiting orientation factor will also be presented in detail in this article.

2. Inverse – Forward kinematic for planar overconstrained CDPR

2.1. Inverse kinematic

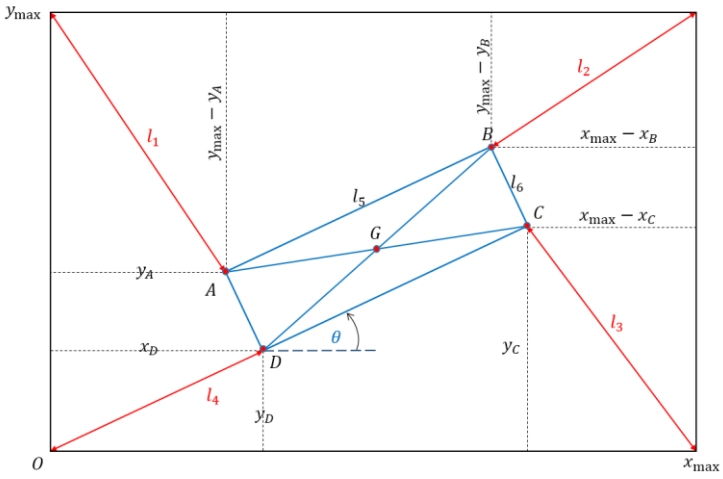

Figure 1. *Kinematic analysis*

The inverse kinematic of the robot is aim to find out the joint's values when the position's values and direction of E-E are known. This problem involves a crucial role in controlling the E-E position. With CDPR, inverse kinematics is generally solved by using the static geometry method from the sketch of the robot. In this paper, inverse kinematics will be resolved in detail by using the geometry solution shown in Figure 1. Due to the restriction of robot DOF, the Oz axis is acceptable to be relaxed inside

each formula. The origin is at point O, and applying geometric knowledge we can deduce the general formula to calculate the length of each cable:

$$\begin{cases} l_1^2 = x_A^2 + \left(y_{\max} - y_A\right)^2 \\ l_2^2 = \left(x_{\max} - x_B\right)^2 + \left(y_{\max} - y_B\right)^2 \\ l_3^2 = \left(x_{\max} - x_C\right)^2 + x_C^2 \\ l_4^2 = x_D^2 + y_D^2 \end{cases} \quad (1)$$

For solving the (1) using parameter θ and coordinate of G (x_G , y_G) which is the E-E position, we have to find the relation between points A(x_A , y_A), B(x_B , y_B), C(x_C , y_C), D(x_D , y_D) and pose θ, x_G , y_G

Finally, the set of equations that express inverse kinematic:

$$\begin{cases} l_1^2 = (x_G - l_{56}\cos(\theta-\alpha))^2 + \left(y_{\max} - y_G + l_{56}\sin(\theta-\alpha)\right)^2 \\ l_2^2 = (x_{\max} - x_G - l_{56}\cos(\theta+\alpha))^2 + \left(y_{\max} - y_G - l_{56}\sin(\theta+\alpha)\right)^2 \\ l_3^2 = (x_{\max} - x_G - l_{56}\cos(\theta-\alpha))^2 + (y_G + l_{56}\sin(\theta-\alpha))^2 \\ l_4^2 = (x_G - l_{56}\cos(\theta+\alpha))^2 + (y_G - l_{56}\sin(\theta+\alpha))^2 \end{cases} \quad (2)$$

where $\alpha = \arctan(\frac{l_6}{l_5})$ and $l_{56} = \frac{\sqrt{l_5^2 + l_6^2}}{2}$

2.2. Forward kinematic

Forward kinematics is the process of calculating the position and orientation of the E-E knowing all the matching joint's variables, namely the lengths of the cables for the configuration of the CDPR type [12].

To calculate the position and orientation of E-E from the set of matching joint's values, for the method proposed in this article, we need to deduce from the system of inverse kinematics equations, based on the existing system of inverse kinematic equation (2), we will obtain a new system of equations that satisfies the requirements of forward kinematics.

Using the set of inverse kinematic equations (2), we can solve the forward kinematics. After withdrawing θ, x_G and y_G , which are a set of parameters defining the position and orientation of E-E, from equations (2), we can deduce the new set of equations. (Notably, sometimes a symbol of $\mathrm{Sin}(x)$ and $\mathrm{Cos}(x)$ will be short as s_x and c_x)

After solving, a set of forward kinematic equations can be expressed as

$$\theta = \operatorname{atan}\frac{s_\theta}{\sqrt{1-s_\theta^2}}; x_G = \frac{\sigma_1 - \sigma_2}{\sigma_3}; y_G = \frac{\sigma_4 - \sigma_5}{\sigma_6} \quad (3)$$

where $s_\theta = \frac{l_1^2 + l_3^2 - (l_2^2 + l_4^2)}{-4l_{56}(x_{\max}s_\alpha - y_{\max}c_\alpha)}$. The symbols σ_1 , σ_2 , σ_3 , σ_4 , σ_5 and σ_6 are used as substitutes. The values of these are expressed as

$$\sigma_1 = (l_1^2 - l_3^2 + x_{\max}^2 - y_{\max}^2 - 2x_{\max}l_{56}c_{(\theta-\alpha)} - 2y_{\max}l_{56}s_{(\theta-\alpha)})(-2y_{\max} + 4l_{56}s_{(\theta+\alpha)})$$

$$\sigma_2 = (-2y_{\max} - 4l_{56}s_{(\theta-\alpha)})(l_2^2 - l_4^2 - x_{\max}^2 - y_{\max}^2 + 2y_{\max}l_{56}s_{(\theta+\alpha)} + 2x_{\max}l_{56}c_{(\theta+\alpha)})$$

$$\sigma_3 = (2x_{\max} - 4l_{56}c_{(\theta-\alpha)})(-2y_{\max} + 4l_{56}s_{(\theta+\alpha)}) - (-2y_{\max} - 4l_{56}s_{(\theta-\alpha)})(4l_{56}c_{(\theta+\alpha)} - 2x_{\max})$$

$$\sigma_4 = (2x_{\max} - 4l_{56}c_{(\theta-\alpha)})(l_2^2 - l_4^2 - x_{\max}^2 - y_{\max}^2 + 2y_{\max}l_{56}s_{(\theta+\alpha)} + 2x_{\max}l_{56}c_{(\theta+\alpha)})$$

$$\sigma_5 = (4l_{56}c_{(\theta+\alpha)} - 2x_{\max})(l_1^2 - l_3^2 + x_{\max}^2 - y_{\max}^2 - 2x_{\max}l_{56}c_{(\theta-\alpha)} - 2y_{\max}l_{56}s_{(\theta-\alpha)})$$

$$\sigma_6 = (2x_{\max} - 4l_{56}c_{(\theta-\alpha)})(-2y_{\max} + 4l_{56}s_{(\theta+\alpha)}) - (-2y_{\max} - 4l_{56}s_{(\theta-\alpha)})(4l_{56}c_{(\theta+\alpha)} - 2x_{\max})$$

3. Limitation for the orientation of end-effector

At each position of E-E, the angle θ will pose different minimum and maximum limitation values. These limit values will never be fixed during the E-E movement in the robot's workspace. When examining in the simulation all the positions that the robot can reach, we can illustrate the concept of orientation limitation.

The limiting angle θ is calculated when we examine each cable length or each joint's value of the robot during operation. Each cable exists γ, which is the angle that was formed in Figure 2. For this robot's configuration, it will consist of 4 angles γ (known as γ_1, γ_2, γ_3 and γ_4). We can assume that $\theta_{\lim}$ the angle θ limitation appeared when γ reach 180^0. $\theta_{\lim}$ can be considered as maxima limitation angle or minima limitation angle or none of them. For this assumption, calculation $\theta_{\lim}$ required some comparisons to choose angles $\theta_{\lim}$ to set θ as maxima ($\theta_{\max}$) and minima ($\theta_{\min}$).

With a random position of E-E on the workspace of the robot, based on this theory, there will be four angles $\theta_{\lim}$ ($\theta_{\lim 1}$, $\theta_{\lim 2}$, $\theta_{\lim 3}$ and $\theta_{\lim 4}$) for this robot's configuration.

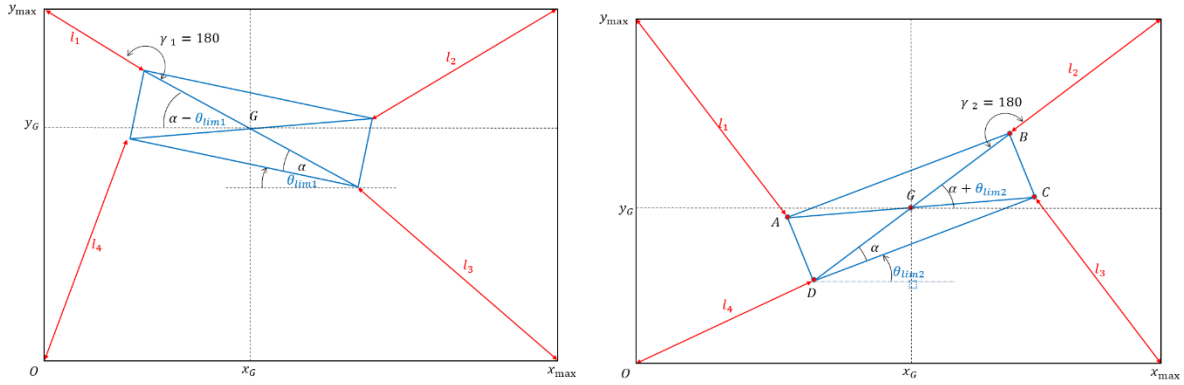

Case γ_1 equal to 180^0 *Case γ_2 equal to 180^0*

Figure 2. *Rotational limitation*

From the above pose, examples are shown in Figure 2, there are four cases where respectively angles γ equal to 180^0. For each case, we can be obtained a formula for the rotational limitations as

$$\begin{cases} \theta_{\lim 1} = \alpha - \tan^{-1}\dfrac{y_{\max} - y_G}{x_G}; \theta_{\lim 2} = \tan^{-1}\dfrac{y_{\max} - y_G}{x_G} - \alpha \\ \theta_{\lim 3} = \alpha - \tan^{-1}\dfrac{y_G}{x_{\max} - x_G}; \theta_{\lim 4} = \tan^{-1}\dfrac{y_G}{x_G} - \alpha \end{cases} \quad (4)$$

Maxima and minima rotational angles θ that E-E can be created by choosing the values which have been compared of $\theta_{\lim 1}$, $\theta_{\lim 2}$, $\theta_{\lim 3}$ and $\theta_{\lim 4}$. By eliminating the maximum and minimum values of

this set, select two values $\theta_{\lim}$ that remain to set as $\theta_{\max}$ and $\theta_{\min}$. Therefore, at each position of E-E, the value θ after calculation must satisfy the condition.

$$\theta \in [\theta_{\min}, \theta_{\max}] \tag{5}$$

The comparison between all $\theta_{\lim}$ values will always change during operation. Due to this calculation, verification, and selection of the limitations θ should depend on the position of E-E.

4. Cable tension distribution algorithm

4.1. Problem in cable tension distribution

Forces act on the E-E shown in Figure 3. The problem of cable tension distribution is to determine the value T_i with i = 1, 2, 3, 4 corresponding to the number of cables. The net of forces created by the tension of each cable can be described in the following form.

$$\mathbf{A\tau = w}_{\mathrm{P}} \tag{6}$$

where $\mathbf{A} \in \mathrm{R}^{3x4}$ is the structure matrix $\mathbf{A} = \begin{bmatrix} \mathbf{u}_1 & \mathbf{u}_2 & \mathbf{u}_3 & \mathbf{u}_4 \\ \mathbf{d}_1 \times \mathbf{u}_1 & \mathbf{d}_2 \times \mathbf{u}_2 & \mathbf{d}_3 \times \mathbf{u}_3 & \mathbf{d}_4 \times \mathbf{u}_4 \end{bmatrix}$, the vector $\boldsymbol{\tau} = \begin{bmatrix} T_1 & T_2 & T_3 & T_4 \end{bmatrix}^{\mathrm{T}} \in \mathrm{R}^{4x1}$ contains values of the tension force of all cables, and $\mathbf{w_P} = \begin{bmatrix} \mathbf{F} & \boldsymbol{\eta} \end{bmatrix}^{\mathbf{T}} \in \mathrm{R}^{3\times1}$ is the matrix which describes the net force created by the tension force of all cables affect to E-E at point G, $\mathbf{F} = \begin{bmatrix} F_x & F_y \end{bmatrix}^{\mathrm{T}} \in \mathrm{R}^{2\times1}$ is external force, and $\eta = M_z \in \mathrm{R}^{1\times1}$ is the momentum about Oz direction. From this robot's configuration, cables could only cause the tensile force which leads to the vector τ as a non-negative vector.

Note that the vector $\vec{u}_i$ in Figure 3 is the unit vector of cable i presented $\begin{bmatrix} u_i^x & u_i^y \end{bmatrix}^{\mathrm{T}} \in \mathrm{R}^{2\times1}$ and the vector $\vec{d}_i$ is the relative position vector from G to A_i can be presented as $\begin{bmatrix} d_i^x & d_i^y \end{bmatrix}^{\mathrm{T}} \in \mathrm{R}^{2\times1}$. Equation (6) is more detail presented as:

$$\begin{bmatrix} u_1^x & u_2^x & u_3^x & u_4^x \\ u_1^y & u_2^y & u_3^y & u_4^y \\ d_1^x u_1^y + d_1^y u_1^x & -d_2^x u_2^y + d_2^y u_2^x & -d_3^x u_3^y - d_3^y u_3^x & d_4^x u_4^y - d_4^y u_4^x \end{bmatrix} \begin{bmatrix} T_1 \\ T_2 \\ T_3 \\ T_4 \end{bmatrix} = \begin{bmatrix} F_x \\ F_y \\ M_z \end{bmatrix} \tag{7}$$

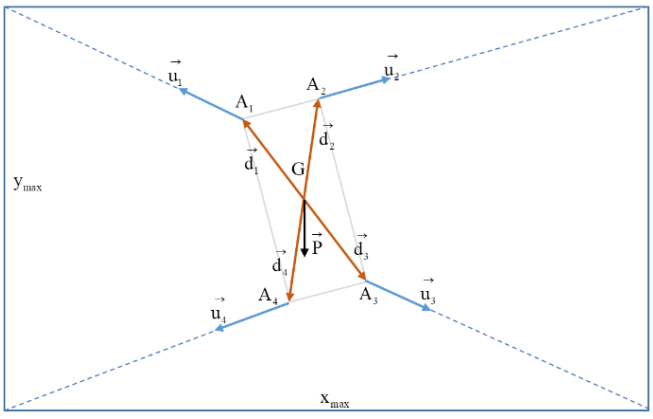

Figure 3. *Force analysis*

The tension force of each cable will be limited by two values of minimum tension force $\underline{\tau} \in \mathrm{R}^{4\times1}$ and maximum $\overline{\tau} \in \mathrm{R}^{4\times1}$, these binding conditions can be expressed as:

$$0_m \le \underline{\tau} \le \tau \le \overline{\tau} \tag{8}$$

where $0_m \in \mathrm{R}^{4\times1}$ is a vector with the value 0.

The problem posed in this paper is to determine how the tension forces of each cable are distributed but still satisfy both (8) and (7).

For this problem, a solution proposed is to select some constraints that can be relaxed. Specifically, for the constraint on the tension limit (8), we can hardly interfere as this shall not be violated to make sure all tensile forces are always positive. But the constraint on the balance of external force (6) is relaxable. A matrix containing the slack variables is proposed to interfere with this constraint, then equation (6) converts to

$$\mathbf{A\tau + s = w_P} \tag{9}$$

where $\mathrm{s} = \begin{bmatrix} \mathrm{s}_1 & \mathrm{s}_2 & \mathrm{s}_3 \end{bmatrix} \in \mathrm{R}^{3\times1}$ is the matrix containing the slack variables s_1, s_2 and s_3 to be added. To ensure the constraint at (9) is always satisfied, it is necessary to calculate to optimize the values s in the objective function of the optimization problem. Based on available tension distribution algorithms, the problem of Linear Programming and Quadratic Programming is the most suitable and adaptive model to solve this problem.

4.2. Quadratic programming – cable tension distribution algorithm

A basic Quadratic Programming problem is proposed and applied to solve the problem of cable tension distribution for the Planar-CDPR robot. There have been many studies and experiments to compare the efficiency between linear programming and quadratic programming for this problem [13-15]. The calculation results of quadratic programming are preferred because of ensuring the continuity of the whole system. The optimal equation containing slack variables and cable tension distribution quantities has the following form.

Minimize: $\mathrm{s}^{\mathrm{T}}\mathrm{D}_1\mathrm{s} + (\tau - \tau^*)^{\mathrm{T}}\mathrm{D}_2(\tau - \tau^*)$ (10)

Subject to: $\mathbf{A\tau + s = w_P}$ and $0_m \le \underline{\tau} \le \tau \le \overline{\tau}$

Where $\mathrm{D}_1 = \begin{bmatrix} \mathrm{d}_{11} & 0 & 0 \\ 0 & \mathrm{d}_{12} & 0 \\ 0 & 0 & \mathrm{d}_{13} \end{bmatrix}$, $\mathrm{D}_2 = \begin{bmatrix} \mathrm{d}_{21} & 0 & 0 & 0 \\ 0 & \mathrm{d}_{22} & 0 & 0 \\ 0 & 0 & \mathrm{d}_{23} & 0 \\ 0 & 0 & 0 & \mathrm{d}_{24} \end{bmatrix}$, $\boldsymbol{\tau}^* = \begin{bmatrix} \mathrm{T}^* & \mathrm{T}^* & \mathrm{T}^* & \mathrm{T}^* \end{bmatrix}^{\mathrm{T}}$

With $\mathrm{D}_1 \in \mathrm{R}^{3\times3}$ and $\mathrm{D}_2 \in \mathrm{R}^{4\times4}$ are weight matrices, which were expressed in the form of diagonal matrices (d_{11}, d_{12}, d_{13}, d_{21}, d_{22}, d_{23} and d_{24} are weight values). Vector $\boldsymbol{\tau}^* \in \mathrm{R}^{4\times1}$ contains the target values for tension force T^*, this value decides the high or low level of tension distribution for each cable.

By selecting $\boldsymbol{\tau}^* \le \underline{\boldsymbol{\tau}}$, the desired tension force with minimum stiffness and power is reached. By selecting $\boldsymbol{\tau}^* = \dfrac{\underline{\boldsymbol{\tau}} + \overline{\boldsymbol{\tau}}}{2}$, the ideal tension force with relative stiffness and power is obtained. Selecting $\tau^* \ge \overline{\tau}$, the solution will lead to the highest tension distribution as well the highest stiffness.

The magnitude of every value D_1 should be chosen higher than values in D_2. For each time compute the optimal distribution force, we will able to determine values of slack variables, the aim that

they will asymptote to zero. However, we can easily set those slack variables by selecting suitable weight matrices D_1 and D_2. The final quadratic optimization problem can be expressed as:

$$\mathbf{f_{min}} = \begin{bmatrix} s_1 \\ s_2 \\ s_3 \end{bmatrix}^T \begin{bmatrix} d_{11} & 0 & 0 \\ 0 & d_{12} & 0 \\ 0 & 0 & d_{13} \end{bmatrix} \begin{bmatrix} s_1 \\ s_2 \\ s_3 \end{bmatrix} + \begin{bmatrix} T_1 - T^* \\ T_2 - T^* \\ T_3 - T^* \\ T_4 - T^* \end{bmatrix}^T \begin{bmatrix} d_{21} & 0 & 0 & 0 \\ 0 & d_{22} & 0 & 0 \\ 0 & 0 & d_{23} & 0 \\ 0 & 0 & 0 & d_{24} \end{bmatrix} \begin{bmatrix} T_1 - T^* \\ T_2 - T^* \\ T_3 - T^* \\ T_4 - T^* \end{bmatrix} \tag{11}$$

From this quadratic programming equation, we will expand and transform it into a general form, by following the steps. First, assume that

$$\mathbf{X} = \begin{bmatrix} x_1 & x_2 & x_3 & x_4 & x_5 & x_6 & x_7 & x_8 \end{bmatrix}^T = \begin{bmatrix} s_1 & s_2 & s_3 & T_1 & T_2 & T_3 & T_4 & 1 \end{bmatrix}^T$$

Finally, the general quadratic optimization form can be written as.

$$f_{min}(X) = X^T \begin{bmatrix} d_{11} & 0 & 0 & 0 & 0 & 0 & 0 & 0 \\ 0 & d_{12} & 0 & 0 & 0 & 0 & 0 & 0 \\ 0 & 0 & d_{13} & 0 & 0 & 0 & 0 & 0 \\ 0 & 0 & 0 & d_{21} & 0 & 0 & 0 & 0 \\ 0 & 0 & 0 & 0 & d_{22} & 0 & 0 & 0 \\ 0 & 0 & 0 & 0 & 0 & d_{23} & 0 & 0 \\ 0 & 0 & 0 & 0 & 0 & 0 & d_{24} & 0 \\ 0 & 0 & 0 & 0 & 0 & 0 & 0 & 4T^{*2} \end{bmatrix} X + \begin{bmatrix} 0 \\ 0 \\ 0 \\ -2T^* \\ -2T^* \\ -2T^* \\ -2T^* \\ 0 \end{bmatrix}^T X \tag{12}$$

Subject to

$$\begin{bmatrix} 1 & 0 & 0 & u_1^x & u_2^x & u_3^x & u_4^x & 0 \\ 0 & 1 & 0 & u_1^y & u_2^y & u_3^y & u_4^y & 0 \\ 0 & 0 & 1 & d_1^x u_1^y + d_1^y u_1^x & d_1^x u_1^y + d_1^y u_1^x & -d_3^x u_3^y - d_3^y u_3^x & d_4^x u_4^y - d_4^y u_4^x & 0 \\ 0 & 0 & 0 & 0 & 0 & 0 & 0 & 1 \end{bmatrix} X = \begin{bmatrix} F_x \\ F_y + P \\ M_z \\ 1 \end{bmatrix} \tag{13}$$

And

$$\begin{bmatrix} 0 & 0 & 0 & -1 & 0 & 0 & 0 & 0 \\ 0 & 0 & 0 & 0 & -1 & 0 & 0 & 0 \\ 0 & 0 & 0 & 0 & 0 & -1 & 0 & 0 \\ 0 & 0 & 0 & 0 & 0 & 0 & -1 & 0 \\ 0 & 0 & 0 & 1 & 0 & 0 & 0 & 0 \\ 0 & 0 & 0 & 0 & 1 & 0 & 0 & 0 \\ 0 & 0 & 0 & 0 & 0 & 1 & 0 & 0 \\ 0 & 0 & 0 & 0 & 0 & 0 & 1 & 0 \end{bmatrix} X \leq \begin{bmatrix} -\underline{\tau} \\ -\underline{\tau} \\ -\underline{\tau} \\ -\underline{\tau} \\ \overline{\tau} \\ \overline{\tau} \\ \overline{\tau} \\ \overline{\tau} \end{bmatrix} \tag{14}$$

5. Offline simulation

Offline simulation is a crucial process that contributes to evaluating the performance of the operations and concepts in this article. As for the problem of tension distribution, many experiments have been carried out to verify more precisely. However, this article is only presented in the form of an offline simulation because it is not eligible to equip the necessary equipment.

To simulate how the Quadratic programming algorithm (12) works, we perform the following steps.

- Selecting the characteristics of the frame: x_{max} = 1 (m), y_{max} = 1 (m)
- Selecting the characteristics of end-effector: l_5 = 0.05 (m), l_6 = 0.2 (m)
- Selecting the limitation of tension force: T_{max} = 20(N), T_{min} = 1 (N)
- Selecting the desired tension parameter in turn at the level of the mechanism reaching:
  1. Case with high stiffness: $T^* = T_{max}$
  2. Case with moderate stiffness: $T^* = \frac{T_{max} - T_{min}}{2}$
  3. Case with low stiffness: $T^* = T_{min}$
- Selecting the start point of E-E: x_G = 0.5 m, y_G = 0.5 m, $\theta = 0^0$
- Assume the external forces that affect E-E with: F_x = 0 (N), F_y = 0 (N), M_z = 0(Nm) - **(**)** (These parameters will be used to verify the result after the simulation)
- Selecting the mass of E-E platform: m = 1 (kg), then $P = mg$ = 9.81 N (g = 9.81 m/s^2)
- Establish the computational parameters for Quadratic Programming: D_{11}=10^{10}, D_{12} =10^{10}, D_{13} =10^{10}, D_{21} =1, D_{22} =1, D_{23} =1, D_{24} =1

After choosing the necessary parameters for the algorithm, we use the MATLAB support tool to solve the Quadratic Programming problem, the results are as follows:

The desired inverse kinematics will produce the path of E-E in the form of a helical loop with the starting point from the center going away (Figure 4). Along with each step of E-E, the cable tension is also modeled according to Figure 5. In addition, to check the accuracy of the algorithm, we will also output the values of the external forces (Figure 6) according to the position of E-E. After observation of the result generated from simulations, the desired tension force $\tau^* \in R^{4\times1}$ is obtained from the maximum stiffness solution (Figure 5-a), each cable will create the tension force which tends to reach the maximum value (20 N). Similar to the case when the desired tension force tend to reach the minimum stiffness solution (Figure 5-c), cable number 2 and 3 sequentially reach the minimum value (1 N) while cable number 1 and 2 tend to keep a moderate force. In Figure 5-b, the desired tension force is set at a medium stiffness level which leads to all cables tending to stand at moderate tension force but also none of them will reach the maximum or minimum like in previous cases. The result gained from the simulation is clear and we can confirm that desired values of tension force affect the stiffness of the mechanism, and also affect the energy consumption and power for the controlling robot. Depending on the usage purpose, carefully choose the desired tension force to ensure power efficiency.

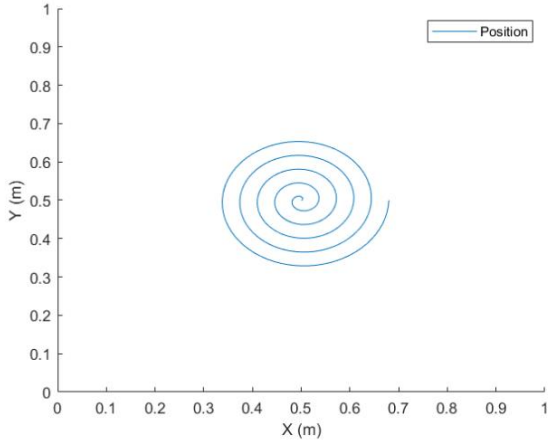

Figure 4. *Positional record*

JTE
HCMUTE
ISSN: 2615-9740

JOURNAL OF TECHNICAL EDUCATION SCIENCE
Ho Chi Minh City University of Technology and Education
Website: https://jte.edu.vn
Email: jte@hcmute.edu.vn

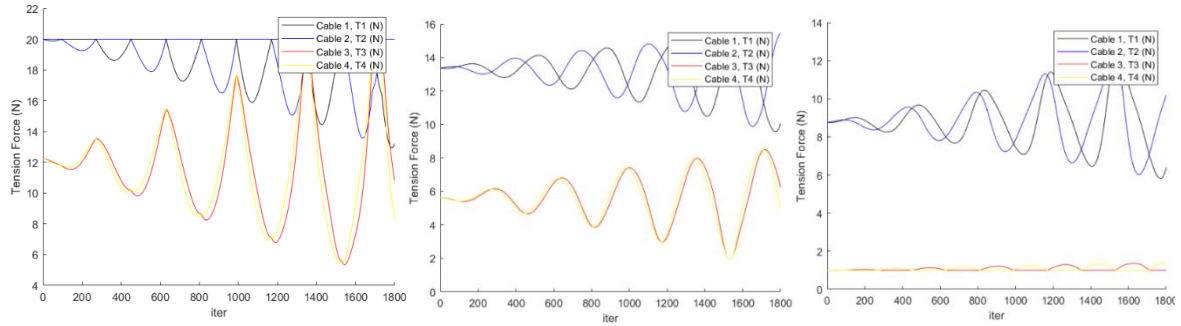

a. Maximum stiffness *b. Medium stiffness* *c. Minimum stiffness*

Figure 5. *Tensional force record*

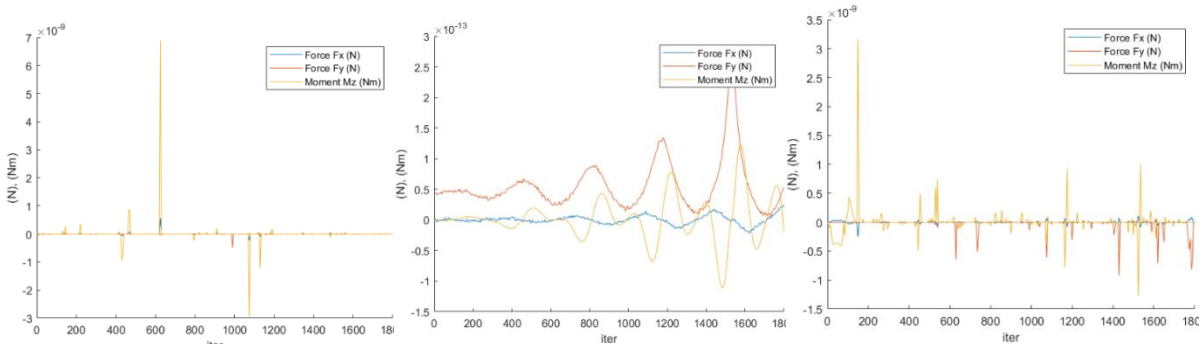

a. Maximum stiffness *b. Medium stiffness* *c. Minimum stiffness*

Figure 6. *External wrench record*

We can see that during E-E spiral moving (Figure 4) simulated for three cases with different desired stiffness, all values of external force always fluctuate around value 0 with an extremely small amplitude (observations can be seen in Figure 6), compared to the initial set value of the external force acting at (**), it is possible to see that the results are completely different from expectations, the reason is that the existence of the slack variables shall create this unnecessary fluctuation. In addition, the noise of the calculation tool has not been taken into account. However, with this extremely small error margin, we can accept the results, in general, the fluctuation value is not significant, but to draw more accurate conclusions, it is necessary to verify the deviation of external forces acting in the entire workspace of the robot.

6. Conclusions

In general, the Quadratic Programming algorithm for calculating the cable tension distribution for the CDPR form has been specifically analyzed to solve the problem of adjusting the stiffness of the robot mechanism. The calculation process is successfully simulated on the MATLAB simulation, the results for the cable tension and the values related to this algorithm are relatively positive, and accurate based on the analysis theory platform. In the process, the article also presented the analysis process and specify solutions to the problem of inverse and forward kinematics for the Planar CDPR form, results were also verified in detail, which is transparent through the above simulation. With this result, it is possible to apply the tension distribution algorithm by Quadratic Programming to the Spatial Cable Driven Parallel robot by changing the parameter matrices optimization problem and the structure matrix in the optimization problem in kinematics. However, there is a disadvantage that the amount of computation will increase significantly, consuming resources of the control device, this suffering later can be overcome by upgrading the control device, but in return, the Spatial form will bring much flexibility, and higher performance than the planar form, and more economic efficiency also. This paper serves as an essential step forward for our further in-depth studies of other complex issues related to our Planar CDPR and Spatial CDPR types in the future.

Acknowledgments

This work was funded by the Ministry of Education and Training of Vietnam, under grant no. B2021-SPK-05, and hosted by Ho Chi Minh City University of Technology and Education, Vietnam.

REFERENCES

[1] S. Qian, B. Zi, W. W. Shang, and Q. S. Xu, "A Review on Cable-driven Parallel Robots," *Chinese Journal of Mechanical Engineering*, vol. 31, no. 1, p. 66, 2018.
[2] T. P. Tho and N. T. Thinh, "An Overview of Cable-Driven Parallel Robots: Workspace, Tension Distribution, and Cable Sagging," *Mathematical Problems in Engineering*, vol. 2022, 2022, Art. no. 2199748.
[3] T. P. Tho and N. T. Thinh, "Using a cable-driven parallel robot with applications in 3D concrete printing," *Applied Sciences*, vol. 11, no. 2, pp. 563, 2021.
[4] C. B. Pham, G. Yang, and S. H. Yeo, "Dynamic analysis of cable-driven parallel mechanisms," in *Proceedings, IEEE/ASME International Conference on Advanced Intelligent Mechatronics*, 2005, pp. 612-617.
[5] S. R. Oh and S. K. Agrawal, "Cable suspended planar robots with redundant cables: Controllers with positive tensions," *IEEE Transactions on Robotics*, vol. 21, no. 3, pp. 457-465, 2005.
[6] P. H. Borgstrom, B. L. Jordan, G. S. Sukhatme, M. A. Batalin, and W. J. Kaiser, "Rapid computation of optimally safe tension distributions for parallel cable-driven robots," *IEEE Transactions on Robotics*, vol. 25, no. 6, pp. 1271-1281, 2009.
[7] P. Liu, Y. Qiu, Y. Su, and J. Chang, "On the minimum cable tensions for the cable-based parallel robots," *Journal of Applied Mathematics*, vol. 2014, 2014, Art. no. 350492.
[8] T. Bruckmann, A. Pott, and M. Hiller, "Calculating force distributions for redundantly actuated tendon-based Stewart platforms," in *Advances in Robot Kinematics*, 2006, pp. 403-412.
[9] H. Li, X. Zhang, R. Yao, J. Sun, G. Pan, and W. Zhu, "Optimal force distribution based on slack rope model in the incompletely constrained cable-driven parallel mechanism of FAST telescope," in *Cable-driven parallel robots*, Springer, Berlin, Heidelberg, 2013, pp. 87-102.
[10] T. Bruckmann, C. Sturm, and W. Lalo, "Wire robot suspension systems for wind tunnels," in *Wind tunnels and experimental fluid dynamics research*, 2010, pp. 29-50.
[11] A. F. Côté, P. Cardou, and C. Gosselin, "A tension distribution algorithm for cable-driven parallel robots operating beyond their wrench-feasible workspace," in *2016 16th International Conference on Control, Automation and Systems (ICCAS)*, 2016, pp. 68-73.
[12] J. P. Merlet, "Solving the Forward Kinematics of a Gough-Type Parallel Manipulator with Interval Analysis," *The International Journal of Robotics Research*, vol. 23, p. 221, 2004.
[13] P. Wolfe, "The Simplex Method For Quadratic Programming," *The Econometric Society*, vol. 27, no. 3, pp. 382-398, 1959.
[14] A. F. Cote, P. Cardou, and C. Gosselin, "A Tension Distribution Algorithm for Cable-Driven Parallel Robots Operating Beyond their Wrench-Feasible Workspace," in 1*6th International Conference on Control, Automation and Systems (ICCAS)*, Oct. 2016, doi: 10.1109/ICCAS.2016.7832301.
[15] E. Picard, S. Caro, F. Plestan, and F. Claveau, "Stiffness Oriented Tension Distribution Algorithm for Cable-Driven Parallel Robots," in *Advances in Robot Kinematics 2020*, Springer, 2020, pp. 209-217.

First Author.

Dao Cong Hoang Kha is a student at Ho Chi Minh City University of Technology and Education, in the academic year 2018 - 2022. He is in the process of completing his graduation thesis at the university. His specialty is Mechatronic in Engineering Technology.

Second Author.

Tuong Phuoc Tho is a Lecturer at the Faculty of Mechanical Engineering at Ho Chi Minh City University of Technology and Education, Viet Nam. He received M.E degree in Manufacturing Technology from Ho Chi Minh University of Technology, Ho Chi Minh, Vietnam, in 2011. His work focuses on Robotics and Mechatronics systems.

Third Author.

Vu Ngoc Duc is a student at Ho Chi Minh City University of Technology and Education, the academic year 2018 - 2022. He is in the process of completing his graduation thesis at the university. His specialty is Mechatronics in Engineering Technology.

Fourth Author.

Nguyen Minh Nhat is a student at Ho Chi Minh City University of Technology and Education, the academic year 2018 - 2022. He is in the process of completing his graduation thesis at the university. His specialty is Mechatronic in Engineering Technology.